# Kinematic Analysis of Robotic Bevel-Gear Trains

F. Freudenstein
R. W. Longman
C.-K. Chen
Columbia University—New York, NY

## Introduction

In robot configurations it is desirable to be able to obtain an arbitrary orientation of the output element or end-effector. This implies a minimum of two independent rotations about two (generally perpendicular) intersecting axes. If, in addition, the output element performs a mechanical task such as in manufacturing or assembly (e.g., drilling, turning, boring, etc.) it may be necessary for the end-effector to rotate about its axis. If such a motion is to be realized with gearing, this necessitates a three-degree-of-freedom, three-dimensional gear train, which provides a mechanical drive of gyroscopic complexity, i.e., a drive with independently controlled inputs about three axes corresponding to azimuth, nutation, and spin.

In a recent article[2] an ingenious bevel-gear train of this type was described, and the article refers to a project headed by Mr. Louis Erwin, Project Coordinator of the Bendix Corporation's Robotics Division, Southfield, Michigan, for the motion of the end-effector of a heavy-duty industrial robot (ML-360).

In this gear train, the orientation of the tool-carrying end-effector is determined by independent rotations about mutually perpendicular, intersecting axes in space, such as occur in the two-gimbal mounts of gyroscopes. In addition, the end-effector can rotate independently about its own axis. In such gear trains the gears and arms rotate about nonparallel axes, which may themselves be rotating about other nonparallel axes.

Various methods for deriving the displacement equations for spur-gear trains can be found in the literature.[1, 3, 6, 7, 8, 9] For these the most systematic approach utilizes the fundamental circuits (obtained directly from the graph of the gear train) from which the displacement equations follow automatically. In bevel-gear trains the analysis is more complex because of the three-dimensional motion of the gears and arms. When arm motion is limited to a rotation about a fixed axis, the displacement equation associated with a fundamental circuit and given in Ref.[4] should be used. In complex epicyclic bevel-gear trains, however, the fundamental circuit equations can no longer be reduced to scalar form, and one would need to monitor the paths of all moving axes, as well as gear and arm rotations. In the following sections a general method for the kinematic analysis of such trains will be developed; first with reference to the previously mentioned robotic bevel-gear train, and thereafter for bevel-gear trains of arbitrary complexity.

## Kinematic Analysis of a Three-Degree-of-Freedom Robotic Gear Train (Fig. 1)

(1) *Kinematic Structure of Gear Train.* The gear train described in, Ref.[2], which is shown in cross section in Fig. 1, has three coaxial input rotations (the rotations of shafts 1, 2, 3 relative to the frame 4). Bevel-gears 1, 2, 5, 6, 7 transmit these rotations to the end-effector attached to gear 7 and housed in arm 8, which pivots on shaft 3. The axis locations of the turning pairs are as follows:

Axis *a*: pairs 1-2, 2-4, 4-3
Axis *b*: pairs 3-5, 3-8, 3-6
Axis *c*: pair 8-7

---

AUTHORS:

**DR. FERDINAND FREUDENSTEIN** *is Higgins Professor of Mechanical Engineering at Columbia University. Besides his academic activities, he has been active in consulting work to industry. His research interests include mechanisms, kinematics, dynamics, and design analysis. Dr. Freudenstein is a member of ASME, the National Academy of Engineering, Harvard Engineering Society, the Columbia Engineering Society and numerous other professional and honorary societies. He has authored over 130 publications and holds nine patents/invention disclosures. He is the winner of numerous professional and academic awards.*

**R.W. LONGMAN** *is on the faculty of Columbia University, doing research in control and dynamics as related to spacecraft and robotics. He also serves on the Board of Directors of the American Astronautical Society and is Managing Editor of their* Journal of the Astronautical Sciences. *He has been visiting professor at MIT, University of Bonn (West Germany), Newcastle (Australia) and Cheng Kung (Taiwan). In addition to his academic work, he has served as a consultant to a number of major corporations and defense contractors. He is a Fellow of the American Astronautical Society and an Associate Fellow of AIAA.*

**C.-K. CHEN** *received his Bachelor of Science Degree from National Taiwan University and his Master of Science from Columbia University. He is presently a graduate research assistant at Columbia, working primarily in the area of mechanisms.*

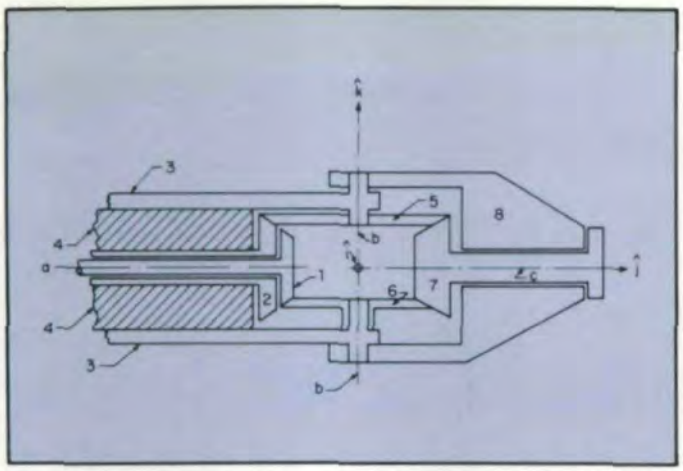

Fig. 1 – Cross section of robotic gear train shown in [2]; "initial" position of gear train

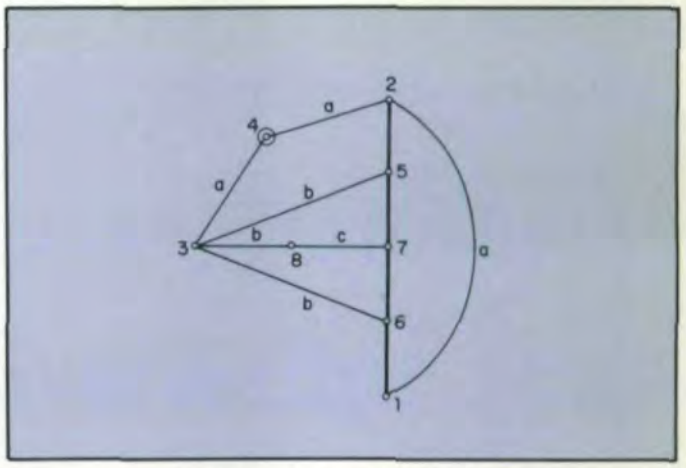

Fig. 2 – Graph of gear train of Fig. 1

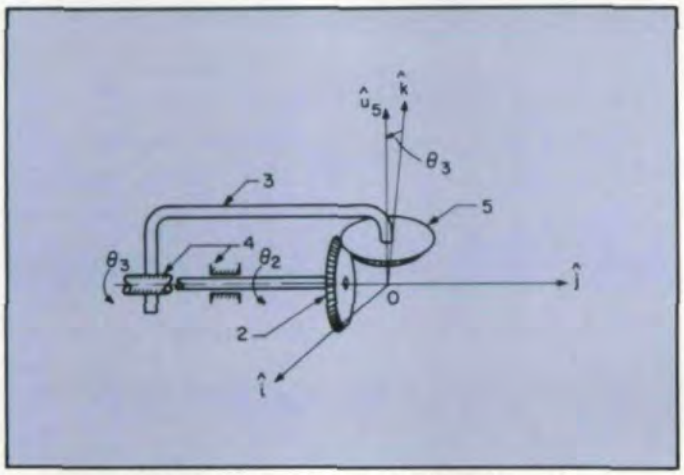

Fig. 3 – Fundamental circuit (2,5)(3) – schematic

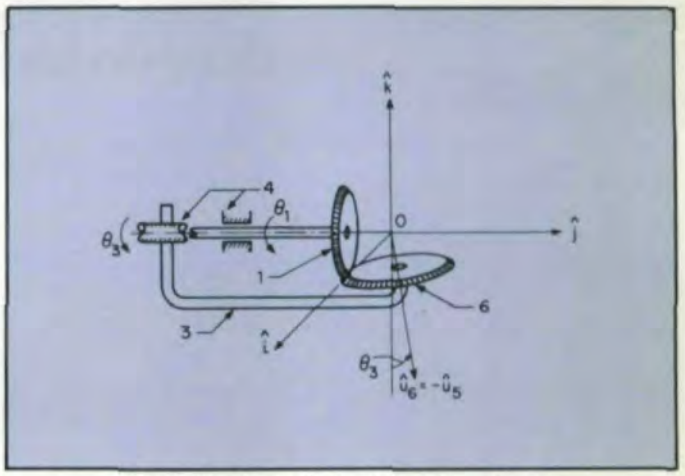

Fig. 4 – Fundamental circuit (1,6)(3) – schematic

The graph of the gear train (in which links are represented by vertices, joints by edges, and the edge connection of vertices corresponds to the joint connection of links) is shown in Fig. 2, in which light edges denote turning pairs and heavier edges denote gear pairs. As can be seen from the graph, the gear train has 8 links, 11 joints (4 gear pairs and 7 turning pairs). The mobility number of the spherical gear train is $\lambda = 3$. The degree of freedom, $F$, of the gear train is obtained from the equation:

$$F = \lambda(l - j - 1) + \Sigma f_i \qquad (1)$$

where $l$, $j$, $f_i$ denote the number of links, joints and freedom of the $i$th joint, respectively. This yields $F = 3(8 - 11 - 1) + 15 = 3$.

From the graph we observe that there are four fundamental circuits: (1,6)(3); (2,5)(3); (6,7)(8); and (5,7)(8). In this notation the first two numbers for each circuit designate the gears, and the last identifies the arm. One special feature of this gear train is evident at this point: since the pitch cones of the gears form a closed configuration, and the angle between the axes of any gear pair is the same (a right angle), it follows that the semi-vertex angle of the pitch cones alternates between complementary values ($\alpha$, say, and, (90 deg $- \alpha$)).

We begin the analysis with the displacement equations associated with each fundamental circuit.

(2) *Fundamental Circuit (2,5)(3).* The fundamental circuit is shown in Fig. 3, including rotations $\theta_2$, $\theta_3$ of shafts 2 and 3, respectively. The positive direction of rotation of shafts 1, 2, and 3 corresponds to a right-handed rotation associated with the unit vector, $\hat{j}$, of the fixed, right-handed, orthogonal triad ($\hat{i}$, $\hat{j}$, $\hat{k}$). The direction of the axis of gear 5 is denoted by the outwardly drawn unit vector, $\hat{u}_5$, and point 0 is the point of intersection of the pitch cones of the gears.

The direction of vector $\hat{u}_5$ is given by

$$\hat{u}_5 = \cos\theta_3 \hat{k} + \sin\theta_3 \hat{i} \qquad (2)$$

The angular displacements associated with the fundamental circuit are derived in Table 1 in terms of the tabular method (sum of displacements with and relative to arm). The number of teeth on gear $i$ is denoted by $N_i$. The vectorial nature of the displacements is evident from the table.

(3) *Fundamental Circuit (1,6)(3).* The fundamental circuit, including the rotation, $\theta_1$, of shaft 1, is shown in Fig. 4. The direction of the axis of gear 6 is denoted by the outwardly drawn unit vector, $\hat{u}_6$, where $\hat{u}_6 = -\hat{u}_5$. The

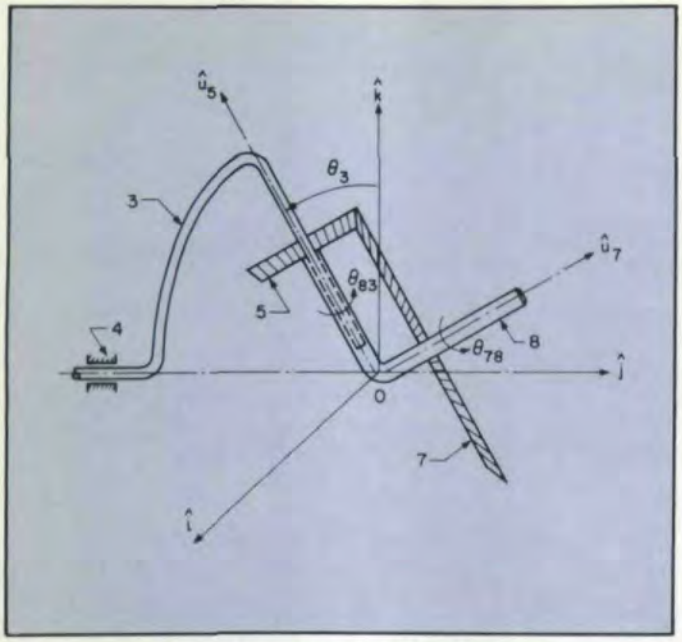


Fig. 5 – Fundamental circuit (5,7)(8) – schematic

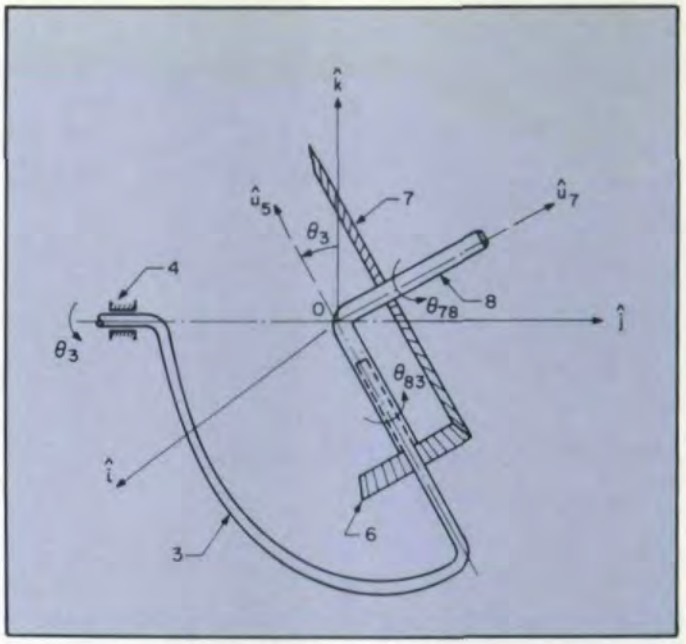


Fig. 6 – Fundamental circuit (6,7)(8) – schematic

angular displacements in this circuit are summarized in Table 2.

(4) *Fundamental Circuit (5,7)(8).* The fundamental circuit is shown in Fig. 5, in which $\theta_{78}$ denotes the angular displacement of gear 7 relative to arm 8 (positive direction defined by a right-handed rotation about unit vector $\hat{u}_7$, the latter outwardly directed along the axis of gear 7); $\theta_{83}$ denotes the angular displacement of arm 8 relative to shaft 3 (positive direction defined by a right-handed rotation about unit vector $\hat{u}_5$). The angular displacements in this circuit are summarized in Table 3. These are functions of the unit vectors $\hat{u}_5$ and $\hat{u}_7$. The latter needs to be determined.

The initial position of arm 8 (see Fig. 1) was taken with its axis coincident with the $j$-axis. The final position of arm 8 is obtained by two successive rotations: a rotation of magnitude $\theta_{83}$ about the $\hat{k}$-axis, followed by a rotation of magnitude $\theta_3$ about the $\hat{j}$-axis. A systematic way of determining the final position of vector $\hat{u}_7$ involves a double application of Rodrigues' equation, one form of which (see for example, F. M. Dimentberg[5]) is as follows:

$$\mathbf{r}' = \mathbf{r}\cos\phi + (1-\cos\phi)\,(\hat{u}\cdot\mathbf{r})\,\hat{u} + (\hat{u}\times\mathbf{r})\sin\phi \qquad (3)$$

In this equation $\mathbf{r}'$ denotes the final position of a vector, $\mathbf{r}$ (the origin of both vectors lying on the axis of rotation), rotating by an angle $\phi$ about an axis, the direction of which is that of unit vector $\hat{u}$.

For the first rotation $\mathbf{r} = \hat{j}$, $\phi = \theta_{83}$ and $\hat{u} = \hat{k}$. This gives

$$\mathbf{r}' = \hat{j}\cos\theta_{83} - \hat{i}\sin\theta_{83}.$$

For the second rotation, we have $\mathbf{r} = \hat{j}\cos\theta_{83} - \hat{i}\sin\theta_{83}$, $\phi = \theta_3$ and $\hat{u} = \hat{j}$. This gives:

$$\hat{u}_7 = \mathbf{r}' = -\sin\theta_{83}\cos\theta_3\,\hat{i} + \cos\theta_{83}\hat{j} + \sin\theta_{83}\sin\theta_3\,\hat{k} \qquad (4)$$

In applying Rodrigues' equation to an open-loop mechanism, such as a robot configuration, it is easiest to start with the open end (the end-effector) and proceed toward the base. In this way, the initial position of all axes is the initial or reference position of the axes (as shown in Fig. 1 for this particular gear train) and the total number of rotations which need to be computed is minimized. It is worth noting that

**Table 1 Angular displacements in fundamental circuit (2,5)(3)***

| Motion | Gear 2 | Gear 5 | Arm 3 |
|---|---|---|---|
| (*a*) Motion with arm | $\theta_3\hat{j}$ | $\theta_3\hat{j}$ | $\theta_3\hat{j}$ |
| (*b*) Motion relative to arm | $\theta_{23}\hat{j}$ | $\frac{N_2}{N_5}\theta_{23}\hat{u}_5$ | 0 |
| Sum (actual motion) | $(\theta_{23}+\theta_3)\hat{j}$ $=\theta_2\hat{j}$ | $\theta_3\hat{j} + \frac{N_2}{N_5}\theta_{23}(\cos\theta_3\hat{k} + \sin\theta_3\hat{i})$ | $\theta_3\hat{j}$ |

*In the tables $\theta_i$ denotes the angular displacement of gear $i$ (relative to ground) and $\theta_{ij}$ the angular displacement of gear $i$ relative to gear $j$ (i.e., $\theta_{ij} = \theta_i - \theta_j$).

**Table 2 Angular displacements in fundamental circuit (1,6)(3)**

| Motion | Gear 1 | Gear 6 | Arm 3 |
|---|---|---|---|
| (*a*) Motion with arm | $\theta_3\hat{j}$ | $\theta_3\hat{j}$ | $\theta_3\hat{j}$ |
| (*b*) Motion relative to arm | $\theta_{13}\hat{j}$ | $\frac{N_1}{N_6}\theta_{13}\hat{u}_6$ | 0 |
| Sum | $(\theta_{13}+\theta_3)\hat{j}$ | $\theta_3\hat{j}-\frac{N_1}{N_6}\theta_{13}\hat{u}_5$ | $\theta_3\hat{j}$ |
| | $=\theta_1\hat{j}$ | $=\theta_3\hat{j}-\frac{N_1}{N_6}\theta_{13}(\cos\theta_3\hat{k}+\sin\theta_3\hat{i})$ | |

**Table 3 Angular displacements in fundamental circuit (5,7)(8)**

| Motion | Gear 5 | Gear 7 | Arm 8 |
|---|---|---|---|
| (*a*) Motion with arm | $\theta_3\hat{j}+\theta_{83}\hat{u}_5$ | $\theta_3\hat{j}+\theta_{83}\hat{u}_5$ | $\theta_3\hat{j}+\theta_{83}\hat{u}_5$ |
| (*b*) Motion relative to arm | $\frac{-N_7}{N_5}\theta_{78}\hat{u}_5$ | $\theta_{78}\hat{u}_7$ | 0 |
| Sum | $\theta_{13}\hat{j}+\left(\theta_{83}-\frac{N_7}{N_5}\theta_{78}\right)\hat{u}_5$ | $\theta_3\hat{j}+\theta_{83}\hat{u}_5+\theta_{78}\hat{u}_7$ | $\theta_3\hat{j}+\theta_{83}\hat{u}_5$ |

**Table 4 Angular displacements in fundamental circuit (6,7)(8)**

| Motion | Gear 5 | Gear 7 | Arm 8 |
|---|---|---|---|
| (*a*) Motion with arm | $\theta_3\hat{j}+\theta_{83}\hat{u}_5$ | $\theta_3\hat{j}+\theta_{83}\hat{u}_5$ | $\theta_3\hat{j}+\theta_{83}\hat{u}_5$ |
| (*b*) Motion relative to arm | $\frac{N_7}{N_6}\theta_{78}\hat{u}_5$ | $\theta_{78}\hat{u}_7$ | 0 |
| Sum | $\theta_3\hat{j}+\left(\theta_{83}+\frac{N_7}{N_6}\theta_{78}\right)\hat{u}_5$ | $\theta_3\hat{j}+\theta_{83}\hat{u}_5+\theta_{78}\hat{u}_7$ | $\theta_3\hat{j}+\theta_{83}\hat{u}_5$ |

since only the relative motions at the joints is needed, the sequence of the finite rotations is immaterial (i.e., the rotation operations are commutative). The angular displacements of this circuit are summarized in Table 3.

(5) *Fundamental Circuit (6,7)(8).* This circuit is shown in Fig. 6 and the angular displacements are summarized in Table 4.

(6) *Compatibility Conditions.* In the angular displacements of the gears in the four fundamental circuits two gears (5 and 6) occur in two fundamental circuits: Gear 5 occurs in circuits (2,5)(3) and (5,7)(8); and gear 6 occurs in circuits (1,6)(3) and (6,7)(8). The angular displacements of each gear, as derived from the two circuits, can now be equated. These are the compatibility conditions which lead to the angular-displacement equations of the gear train.

From Tables 1 and 3, the compatibility condition for gear 5 is the following:

$$\frac{N_2\theta_{23}}{N_5}\sin\theta_3\hat{i}+\theta_3\hat{j}+\frac{N_2\theta_{23}}{N_5}\cos\theta_3\hat{k}$$
$$=\left(\theta_{83}-\frac{N_7}{N_5}\theta_{78}\right)\sin\theta_3\hat{i}+\theta_3\hat{j}+\left(\theta_{83}-\frac{N_7}{N_5}\theta_{78}\right)\cos\theta_3\hat{k} \qquad (5)$$

where

$$\theta_{83}-\frac{N_7}{N_5}\theta_{78}=\frac{N_2\theta_{23}}{N_5} \qquad (6)$$

Similarly, using Tables 2 and 4, the compatibility condition for gear 6 is:

$$-\frac{N_1}{N_6}\theta_{13}\sin\theta_3\hat{i}+\theta_3\hat{j}-\frac{N_1}{N_6}\theta_{13}\cos\theta_3\hat{k}$$
$$=\left(\theta_{83}+\frac{N_7}{N_6}\theta_{78}\right)\sin\theta_3\hat{i}+\theta_3\hat{j}+\left(\theta_{83}+\frac{N_7}{N_6}\theta_{78}\right)\cos\theta_3\hat{k} \qquad (7)$$

where

$$-\frac{N_1}{N_6}\theta_{13}=\theta_{83}+\frac{N_7}{N_6}\theta_{78} \qquad (8)$$

(7) *The Displacement Equations.* The angular-velocity ratio of a pair of bevel-gears, $i$, $j$, with semivertex angles $\alpha_i$ and $\alpha_j$, respectively, and rotating about fixed axes with angular velocities $w_i$ and $w_j$, respectively, is given by

$$\frac{\omega_i}{\omega_j}=\frac{\sin\alpha_i}{\sin\alpha_j} \qquad (9a)$$

In view of the right angle between the axes of the gears, $\alpha_i = 90 \text{ deg} - \alpha_j$, so that

$$\tan\alpha_j=\frac{\omega_i}{\omega_j}=\frac{N_j}{N_i} \qquad (9b)$$

Hence, if $\alpha$ denotes the semivertex angle of the pitch cone of gear 1, it follows that

$$\tan\alpha=N_1/N_6=N_2/N_5 \qquad (10a)$$

and that

$$1/\tan\alpha=N_6/N_7=N_5/N_7 \qquad (10b)$$

Substituting equations (10$a$,$b$) into the compatibility equations (6) and (8), respectively, we have

$$-\theta_{78}\tan\alpha+\theta_{83}=\theta_{23}\tan\alpha \qquad (11)$$

and

$$\theta_{78}\tan\alpha+\theta_{83}=-\theta_{13}\tan\alpha \qquad (12)$$

This yields

$$\theta_{78}=-\frac{1}{2}(\theta_1+\theta_2-2\theta_3) \qquad (13)$$

and

$$\theta_{83}=\frac{1}{2}(\theta_2-\theta_1)\tan\alpha \qquad (14)$$

Substituting Equation 14 into Equation 4 for $\hat{u}_7$ we obtain the orientation of the end-effector, which is

$$\hat{u}_7=-\sin\left[\frac{1}{2}(\theta_2-\theta_1)\tan\alpha\right]\cos\theta_3\hat{i}$$
$$+\cos\left[\frac{1}{2}(\theta_2-\theta_1)\tan\alpha\right]\hat{j}$$
$$+\sin\left[\frac{1}{2}(\theta_2-\theta_1)\tan\alpha\right]\sin\theta_3\hat{k} \qquad (15)$$

Equations 13-15 give the orientation of the end-effector and its angular displacement as a function of the rotations of the input shafts.

## Discussion

The angular displacements of all gears as a function of input rotations follows directly from the tables with the aid of Equations 13-15. Equations 13-15 support the statements made in Ref.[2]. We find that:

(*a*) When the internal shafts 1 and 2 rotate equally in opposite directions, arm 8 pivots about the wrist axes of gears 5 and 6 and $\hat{u}_7 = \hat{j}$.

(*b*) If shafts 1 and 2 are stationary, the entire assembly rotates with shaft 3, the end-effector rotating at twice the speed of shaft 3.

(*c*) If shafts 1 and 2 rotate equally in the same direction, the end-effector rotates in its bearings in arm 8, the position of which is determined by shaft 3.

Variation of the pitch-cone semivertex angle, $\alpha$, can serve to increase or decrease the magnitude of the angular displacements of the end-effector relative to those of the input shafts.

## A General Procedure for the Kinematic Analysis of Complex Bevel-Gear Trains

In light of the analysis which has just been given a sequential, multi-step procedure applicable to the kinematic analysis of general, complex bevel-gear trains can be formulated as follows:

(*a*) Determine the graph (i.e., the kinematic structure) of the gear train, its degree of freedom and any special restrictions on dimensions (such as, the closure of the pitch cones).

(*b*) Determine the fundamental circuits of the gear train.

(*c*) Derive the angular-displacement equations for each fundamental circuit, keeping track not only of the arm and gear rotations, but also of the moving axes of these members. In the case of gear trains of gyroscopic complexity (i.e., gear trains in which one or more arms can rotate about two nonparallel, intersecting axes) the general displacement equations for a fundamental circuit are derived in the Appendix. In the

**Table 5 Angular displacements of gears and arm in a fundamental circuit of gyroscopic complexity**

| Motion | Gear 1 | Gear 2 | Arm 3 |
|---|---|---|---|
| (*a*) Motion with arm | $\theta\hat{k}$ $+\phi\hat{a}$ | $\theta\hat{k}$ $+\phi\hat{a}$ | $\theta\hat{k}$ $+\phi\hat{a}$ |
| (*b*) Motion relative to arm | $\frac{N_2}{N_1}\psi\hat{a}$ | $\psi\hat{s}$ | 0 |
| Sum | $\theta\hat{k}+\left(\phi+\frac{N_2}{N_1}\psi\right)\hat{a}$ | $\theta\hat{k}+\phi\hat{a}+\psi\hat{s}$ | $\theta\hat{k}+\phi\hat{a}$ |

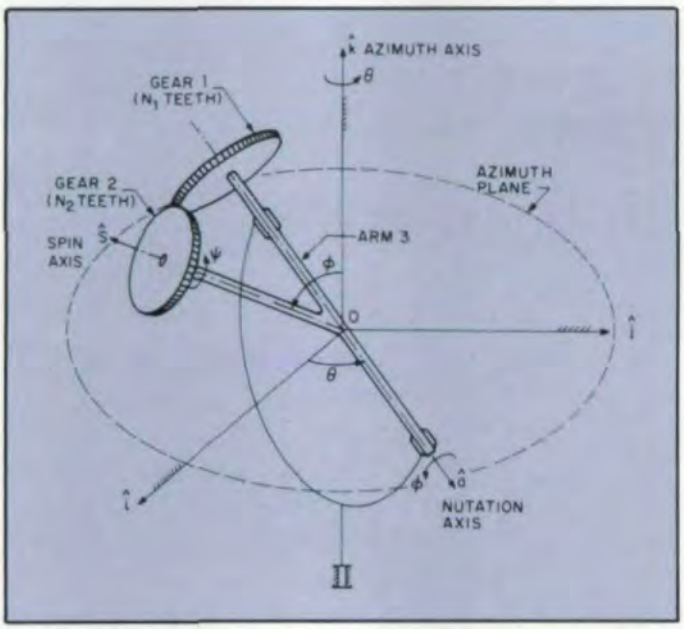


Fig. 7—Fundamental circuit of a bevel-gear pair the motion of which is of gyroscopic complexity

case of gear trains of greater complexity (e.g., those in which the arm can rotate about an arbitrary number of nonparallel, intersecting axes), the fundamental-circuit equation can be derived generally along similar lines by means of the multiple application of Rodrigues' theorem.

(*d*) Determine the compatibility equations from the fundamental circuit equations.

(*e*) Determine the displacement equations from the compatibility equations.

## Conclusion

The analysis of a robotic, three-degree-of-freedom bevel-gear train has been developed in detail and a general procedure outlined, which, with a multiple application of Rodrigues' theorem, yields a general and systematic procedure for the kinematic analysis of bevel-gear trains of arbitrary complexity, such as occur in three-dimensional applications, including robotics. The procedure can be readily computerized.

## Appendix

*The Displacement Equations for a Fundamental Circuit of a Bevel-Gear Pair in a Bevel-Gear Train of Gyroscopic Complexity.* We consider the general circuit consisting of bevel-gears 1, 2, arm 3 and the gimbal mount of the arm, as shown in Fig. 7.

A fixed, right-handed, Cartesian coordinate system associated with unit vectors $\hat{i}$, $\hat{j}$, $\hat{k}$ and with $\hat{\imath}$, $\hat{\jmath}$ in the horizontal (or azimuthal) plane is shown with origin at the point of intersection of the pitch cones of the bevel gears. The rotation of the arm is composed of the rotation, $\phi$, about the nutation axis (directed along unit vector $\hat{a}$) and rotation, $\theta$, about azimuth axis, $\hat{k}$. All rotations are defined in the right-handed sense about their respective axes. Gears 1 and 2 have $N_1$ and $N_2$ teeth, respectively, and the rotation of gear 1 relative to the arm about the spin axis (unit vector $\hat{s}$) is $\psi$. The azimuth, nutation, and spin axes are indicated in the figure.

The angular displacements of the gears and arm can be obtained by considering the motion relative to and with the arm, as given in Table 5. In addition, we need to keep track of the positions ($\hat{k}$, $\hat{a}$, $\hat{s}$) of the azimuth, nutation, and spin axes. Vector $\hat{k}$ is fixed, and vector $\hat{a}$ is given by:

$$\hat{a}=\cos\theta\hat{i}+\sin\theta\hat{j} \tag{A1}$$

Vector $\hat{s}$ is obtained from a double application of Rodrigues' equation.[3] In the first rotation $\mathbf{r}=\hat{k}$, $\phi=\phi$, $\hat{u}=\hat{i}$ and $\mathbf{r}'=\hat{k}\cos\phi-\hat{j}\sin\phi$; and in the second rotation $\mathbf{r}=\hat{k}\cos\phi-\hat{j}\sin\phi$, $\phi=\theta$ and $\hat{u}=\hat{k}$. This gives:

$$\hat{s}=\mathbf{r}'=\sin\phi\sin\theta\hat{i}-\sin\phi\cos\theta\hat{j}+\hat{k}\cos\phi \tag{A2}$$

Substituting equations (A1, A2) into the resultant displacements shown in Table 5, we obtain the angular displacements of the gears relative to the fixed unit triad ($\hat{i}$, $\hat{j}$, $\hat{k}$) as follows:

*Position of gear 1:*

$$\left(\frac{N_2}{N_1}\psi+\phi\right)\cos\theta\hat{i}+\left(\frac{N_2}{N_1}\psi+\phi\right)\sin\theta\hat{j}+\theta\hat{k} \tag{A3}$$

*Position of gear 2:*

$$(\phi\cos\theta+\psi\sin\phi\sin\theta)\hat{i}+(\phi\sin\theta-\psi\sin\phi\cos\theta)\hat{j}+(\theta+\psi\cos\phi)\hat{k} \tag{A4}$$

*Position of arm 3:*

$$\phi\cos\theta\hat{i}+\phi\sin\theta\hat{j}+\theta\hat{k} \tag{A5}$$

*(continued on page 48)*

## KINEMATIC ANALYSIS OF ROBOTICS . . .

*(continued from page 13)*

**References**

1. ALLEN, R. R., "Multiport Models for the Kinematic and Dynamic Analysis of Gear Power Transmission," ASME *Journal of Mechanical Design*, Vol. 101, No. 2, Apr. 1979, pp. 258-267.
2. ANONYMOUS, "Bevel Gears Make Robot's 'Wrist' More Flexible," *Machine Design*, Vol. 54, No. 18, Aug. 12, 1982, p. 55.
3. BUCHSBAUM, F., and FREUDENSTEIN, F., "Synthesis of Kinematic Structure of Geared Kinematic Chains and Other Mechanisms," *J. Mechanisms and Machine Theory*, Vol. 5, 1970, pp. 357-392.
4. DAY, C. P., AKEEL, H. A., and GUTKOWSKI, L. J., "Kinematic Design and Analysis of Coupled Planetary Bevel-Gear Trains," ASME *Journal of Mechanisms, Transmissions, and Automation in Design*, Vol. 105, No. 3, Sept. 1983, pp. 441-445.
5. DIMENTBERG, F. M., "Determination of the Positions of Spatial Mechanisms," (Russian), *Izdat. Akad. Nauk*, Moscow, 1950.
6. FREUDENSTEIN, F., "An Application of Boolean Algebra to the Motion of Epicyclic Drives," ASME *Journal of Engineering for Industry*, Vol. 93, 1971, pp. 176-182.
7. FREUDENSTEIN, F., and YANG, A. T., "Kinematics and Statics of a Coupled Epicyclic Spur-Gear Train," *J. Mechanisms and Machine Theory*, Vol. 7, 1972, pp. 263-275.
8. MERRITT, H. E., *Gear Trains*, Pitman and Sons, London, 1947.
9. POLDER, J. W., *A Network Theory of Variable Epicyclic Gear Trains*, Eindhoven, Greve Offset, 1969.
10. YANG, A. T., and FREUDENSTEIN, F., "Mechanics of Epicyclic Bevel-Gear Trains," *ASME Journal of Engineering for Industry*, Vol. 95, 1973, pp. 497-502.

*The authors are grateful to the General Motors Research Laboratories for the support of this research through a grant to Columbia University.*

*This article was previously presented at the ASME Design Engineering Technical Conference, October 1984. Paper No. 84-Det-22.*

## CURVIC COUPLING DESIGN . . .

*(continued from page 46)*

to keep the clutch teeth in engagement or to move them out of engagement. Higher pressure angles are often used for shift clutches to obtain a proportionately wider space between the toplands of teeth for easy engagement.

The tooth contact of non-generated clutch teeth with positive pressure angle will move very quickly to the edge of the tooth at the heel as the clutch is disengaged under load. To obtain proper tooth contact at all depths of engagement, a generated helical surface should be used. For the great majority of small clutches which shift under load, however, it is entirely satisfactory to design both members with identical convex teeth. When both members are convex, the localized tooth contact remains safely positioned on the surface of the teeth at all depths of engagement thus approximating the action of a helical surface.

Since this localized tooth contact travels from toe to heel as the teeth are disengaged, the amount of this bearing shift should be calculated.

$$\Delta S_L = \frac{h_o}{2} \tan \phi \frac{r_c}{A}$$

where $\Delta S_L$ = bearing shift lengthwise on the tooth

$h_o$ = contact depth

$\phi$ = pressure angle

$r_c$ = cutter radius

$A$ = mean radius of coupling

This calculated amount of bearing shift should be compared with the available face width as follows:

$$\Delta S_L = F - \tfrac{1}{2}\sqrt{\frac{r_c}{1000}}$$

where $F$ = face width

The shift clutch diameter which has been determined in a previous section should be checked according to the formula below. This applies to case-hardened teeth which shift under load and the calculated stress should not exceed 150,000 psi. maximum at operating temperatures.

$$s_c = \frac{0.9T}{AF\,h_o}$$

where $s_c$ = surface stress, psi.

$T$ = torque, lbs. inches

$A$ = mean radius of clutch, inches

$F$ = face width, inches

$h_o$ = contact depth

For clutches which shift under stationary no-load conditions, the surface stress should not exceed 40,000 psi. for case-hardened steel, as given by the following formula:

$$s_c = \frac{T}{AFN\,h_o}$$

The standard tooth proportions given in an earlier section are suggested for initial use in designing shift and overload clutches.

* * *

## MIRROR FINISHING OF TOOTH SURFACES . . .

*(continued from page 26)*

8. OPITZ, H., and GÜHRING, K., "High Speed Grinding", *Annals of CIRP*, Vol. 16, 1968, p. 61-73.
9. ISHIBASHI, A., "The Characteristic of Circular-Arc-Toothed Cylindrical Gears", *Bull. Japan Soc. Mech. Engrs.*, Vol. 9, No. 33, Feb. 1966, p. 200-208.

*The authors express their thanks to Emeritus Profs. A. Wakuri and T. Ueno, Kyushu University, for their encouragement. They are also indebted to the staff of the Machine Shop of the Faculty of Science and Engineering, Saga University, for making the gear grinder used in this investigation.*

*This article was previously presented during the November, 1984 ASME Technical Conference. Paper no. 84-DT-153.*